Mathematical Modeling of Debye Temperature, Vickers Hardness, and Interatomic Bonding Behavior in CoNbSn and FeNbSn Half-Heusler Alloys under High Hydrostatic Compression up to 80 GPa

S. Azra [a], N.H. Fares [b,d] AND F. Fares [c,d]

[a] Department of Mathematics, Faculty of Mathematics and Computer Science, University Mohamed El-Bachir El-Ibrahimi of Bordj- Bou- Arreridj, 34000, Algeria.
[b] Department of Informatics, Faculty of Mathematics and Computer Science, University Mohamed El-Bachir El-Ibrahimi of Bordj- Bou- Arreridj, 34000, Algeria.
[c] Electronics Department, Faculty of Science, University Mohamed El-Bachir El-Ibrahimi of Bordj- Bou- Arreridj, 34000, Algeria.
[d] Laboratory of Materials Physics and Its Applications, University of M'sila, 28000 M'sila, Algeria

Email: souad.azra@univ-bba.dz

Received: 12/04/2025, Accepted: 27/09/2025

Abstract

The present study focuses on the mathematical modeling and quantitative analysis of the impact of high hydrostatic compression, up to 80 GPa, on key thermomechanical properties of hypothetical half-Heusler compounds with a Niobium base atom, specifically CoNbSn and FeNbSn. Using elastic constants and structural parameters as reported in *Revista Mexicana de Física*, 70(4), 041002 (2024), we derive pressure-dependent behaviors of sound velocities, Debye temperature, minimum thermal conductivity, Vickers hardness, and Cauchy pressure. At zero pressure, our computed values for Vickers hardness and Debye temperature are 11.12 GPa and 395.5 K for CoNbSn, and 9.35 GPa and 409.2 K for FeNbSn, respectively. The analytical results indicate a monotonic increase in thermal conductivity, Debye temperature, and hardness as pressure increases, reaching maximal values at 80 GPa. Conversely, the Cauchy pressure *Cp* exhibits a nonlinear and strictly decreasing trend with increasing pressure for both compounds. These trends are described using pressure-dependent mathematical models derived from the elastic tensor components, highlighting the interplay between mechanical stability and pressure-induced structural behavior in XNbSn (X = Co, Fe) systems.

Keywords: XNbSn (X= Co, Fe) Half-Heusler alloys, High-pressure, Debye temperature, Vickers hardness.

1. INTRODUCTION

Materials science continues to serve as a foundational pillar for the development of advanced materials that meet the ever-growing technological demands of modern society. Among these, Half-Heusler (HH) compounds have emerged as promising candidates for thermoelectric applications due to their ability to convert waste heat into usable electrical energy. Within this context, several recent studies have employed computational and mathematical modeling techniques to explore the multifaceted properties of HH alloys.

Giri et al. [1] utilized semi-classical Boltzmann Transport Theory (BTE), in conjunction with Density Functional Theory (DFT), to analyze the structural, electronic, magnetic, and thermoelectric behavior of XNiAs (X = Sc, Y) compounds. Similarly, Islam and Sheikh [2] conducted first-principles calculations based on DFT to investigate various physical properties of XCrAl (X = Fe, Co, Ni, Cu) HH alloys, with an emphasis on their potential for high-temperature applications. Gu et al. [3] further extended this line of inquiry by studying the effects of hydrostatic pressure on the phase stability, structural parameters, and electronic, elastic, and thermodynamic properties of the NiVSb half-Heusler compound.

In a related study, Osafile and Nenuwe [4] employed DFT-based first-principles calculations to model the lattice dynamics and thermodynamic responses of XNbSn (X = Co, Rh, Ir) half-Heusler semiconductors. Their results confirm that the XNbSn alloys crystallize in a face-centered cubic (FCC) structure, with space group F-43m and number 216, which is characteristic of many stable HH phases. More recently, Shabara and Alsobhi [5] used the full-potential linearized augmented plane wave plus local orbitals method (FP-(L)APW + lo), within the framework of DFT, to analyze the influence of hydrostatic pressure on the elastic properties of hypothetical XNbSn (X = Cr, Mn, Co, Fe, V) compounds.

Building upon these studies, the present work focuses on the mathematical modeling of pressure-dependent behaviors in two hypothetical half-Heusler alloys with a niobium base atom: CoNbSn and FeNbSn. Specifically, we investigate the evolution of mass density ρ, sound velocities v_m , Debye temperature θ_D , minimum thermal conductivity k_{min} , Vickers hardness H_v , and Cauchy pressure Cp , using the pressure-dependent elastic constants and structural parameters reported by Shabara and Alsobhi [5]. The modeling approach integrates elasticity theory with thermodynamic relations and empirical hardness models, offering a comprehensive mathematical description of how these key material properties evolve under high-pressure conditions (up to 80 GPa).

2. THEORETICAL MODELS AND DISCUSSION OF RESULTS

2.1. Mass density

The experimental mass density ρ of substance is defined as the mass divided by the volume. The theoretical mass density of crystal substance is related to the structure and its chemical composition, it is given as follows [6, 7] :

$$\rho = \frac{z.M}{(a.b.c.\sqrt{\sin^2\alpha+\sin^2\beta+\sin^2\gamma-2(1-\cos\alpha.\cos\beta.\cos\gamma)})N_A} \quad (1)$$

where z is the number of formula units in unit cell, M is the molecular weight of a formula unit, a, b, and c are unit cell axes lengths, N_A is the Avogadro constant, and α, β and γ are unit cell axes angles.

Using the structural parameters reported by Shabara and Alsobhi [5], the calculated mass density at different values of pressure for CoNbSn and FeNbSn substances are plotted in figure

1. The mass density of both CoNbSn and FeNbSn increases when the pressure increase (volume is compressed) [7, 8]. This behavior for ρ was qbserved also found in wurtzite cadmium sulfide (w-CdS) [8]. At p = 0 GPa, the mass density ρ of CoNbSn is 9.191 g/cm^3, while that of FeNbSn is 7.934 g/cm^3, respectively.

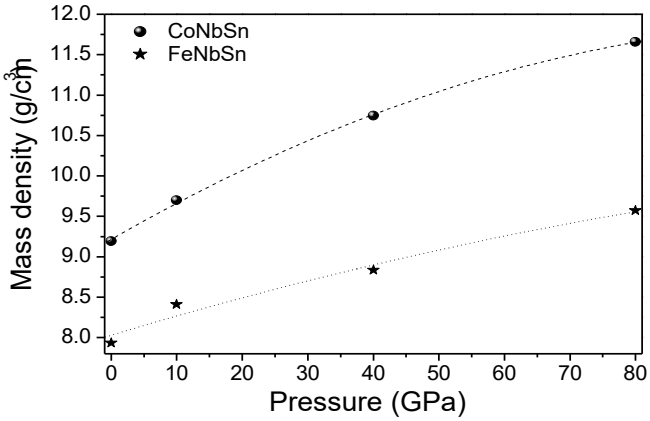

Fig. 1 – Mass density of CoNbSn and FeNbSn substances versus pressure up to 80 GPa.

2.2. Sound velocity

Based on the elastic constants of single crystal, the phase velocities of the pure longitudinal and transverse modes can be calculated [9, 10]. For different crystal classes, the average sound velocity v_m may be usually calculated using the following equation [4]:

$$v_m = \left[\frac{1}{3}\left(\frac{2}{v_t^3} + \frac{1}{v_l^3}\right)\right]^{-1/3} \qquad (2)$$

where v_l is the longitudinal acoustic velocity and v_t is the transverse acoustic velocity, respectively.

The longitudinal v_l and transverse v_t acoustic wave velocities can be obtained from the bulk modulus B, the shear modulus G and the mass density ρ using Eqs (3) and (4), respectively [4]:

$$v_l = \sqrt{\frac{1}{\rho}\left(B + \frac{4}{3}G\right)} \qquad (3)$$

$$v_t = \sqrt{\frac{G}{\rho}} \qquad (4)$$

At different values of pressure, the calculated sound velocities v_l, v_t and v_m are plotted in figure 2 for CoNbSn compound, and in figure 3 for FeNbSn, respectively. The sound velocity of both CoNbSn and FeNbSn increases when the pressure increased from 0 to 80 GPa, this increasing of the sound velocity is due to vibrational excitations originating from the acoustic modes at low temperatures [8]. The calculated zero-pressure sound velocities v_l, v_t and v_m for CoNbSn material are: 5502, 3119, and 3468 m/s, respectively, while these of FeNbSn material are: 5858, 3244, and 3614 m/s, respectively. Our calculated zero-pressure v_l, v_t and v_m for

CoNbSn material are in good agreement with the theoretical values (5435.5, 3020.3, and 3354 m/s, respectively) reported by Osafile and Nenuwe [4]. Furthermore, our calculated v_m (3468 m/s) for CoNbSn is localized between the values 3317.41 m/s and 3512.99 m/s reported by Wafula and co-authors [11].

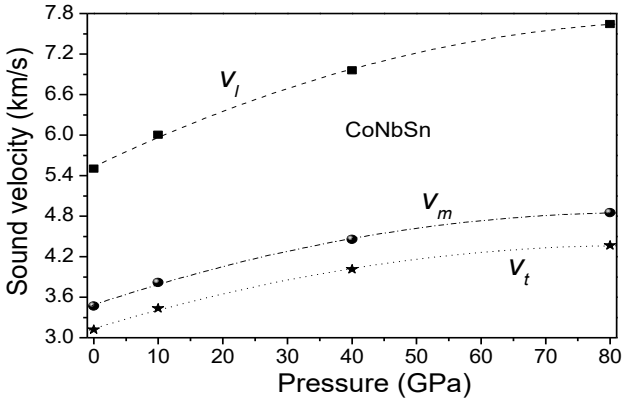

Fig. 2 – Impact of high-pressure up to 80 GPa on the sound velocities v_l, v_t and v_m for CoNbSn Half-Heusler compound.

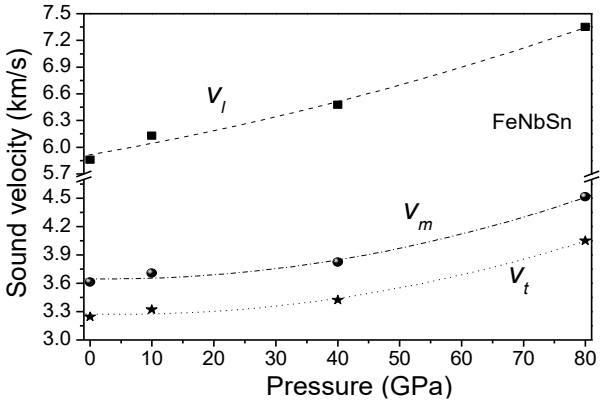

Fig. 3 – Sound velocities v_l, v_t and v_m for FeNbSn material versus pressure up to 80 GPa.

2.3. Debye temperature

The Debye temperature θ_D is a fundamental thermophysical property of solids, it represents the temperature at which the vibrational energy of atoms within the solid material equals their thermal energy [12]. The Debye temperature θ_D connects with several physical qyantities, sunch as interatomic bonding, thermal expansion coefficient, thermal conductivity, highest allowed phonon frequency, lattice vibration, melting temperature,...etc [13-17]. Upon the acquisition of the speed of the sound v_m, the Debye temperature θ_D may be obtained using the following usuel equation [11, 16]:

$$\theta_D = \frac{h}{k_B}\left[\left(\frac{3nN_A\rho}{4\pi M}\right)\right]^{1/3} v_m \qquad (5)$$

where h is the Plank's constant, n the number of atoms in a molecule, N_A is the Avogadro number, ρ is the mass density, k_B is the Boltzmann's constant and M is the molecular weight.

At zero-pressure, the Debye temperature for FeNbSn material is 409.2 K, slightly higher, compared to CoNbSn, which has a lower θ_D of around 395.5 K. Although, this later value is higher than the theoretical one (θ_D = 343 K) obtained (at p = 0 GPa and T = 0 K) from the quasi-harmonic Debye model, reported by Toher and co-authors [18], it is in good agreement with the theoretical values (θ_D = 382.44 K) [4] and (θ_D = 378.59 K, 409.04 K) [11]. The deviation between the two values: θ_D = 395.5 and 409.04 K is only around 3.31%. The calculated Debye temperature θ_D at different values of pressure (p = 0, 10, 40 and 80 GPa) for both CoNbSn and FeNbSn hypothetical half-Heusler materials are grouped in Table 1 and plotted in figure 4.

Table 1 – Calculated Debye temperature θ_D at different pressure (p = 0, 10, 40 and 80 GPa) for both CoNbSn and FeNbSn materials, [a]-Ref. [4], [b]-Ref. [11] GGA, [c]-Ref. [11] LDA, [d]-Ref. [18].

Pressure (GPa)	0	10	40	80
CoNbSn	395.5, 382.44[a], 378.59[b], 409.04[c], 343[d]	443.1	535.3	598.9
FeNbSn	409.2	427.9	448.9	544.3

As for several materials [13-17], the Debye temperature θ_D of both CoNbSn and FeNbSn substances increases when the pressure increase. This behaviour can be attributed to the influence of pressure on the interatomic interactions and electronic structure in the solid [19]. The behavior in this case is very similar to that found in calcium oxide [13] and gallium antimonide (GaSb) [14] and Mg_2Ni binary material [19]. According to Fig. 4, the polynomial fits of the Debye temperature θ_D (in K) as a function of pressure p (in GPa) are as follows:

$$\theta_D = 397.67 + 4.45p - 2.42 \times 10^{-2}p^2 \text{ (for CoNbSn)} \quad (6)$$

$$\theta_D = 414.87 + 0.28p + 1.66 \times 10^{-2}p^2 \text{ (for FeNbSn)} \quad (7)$$

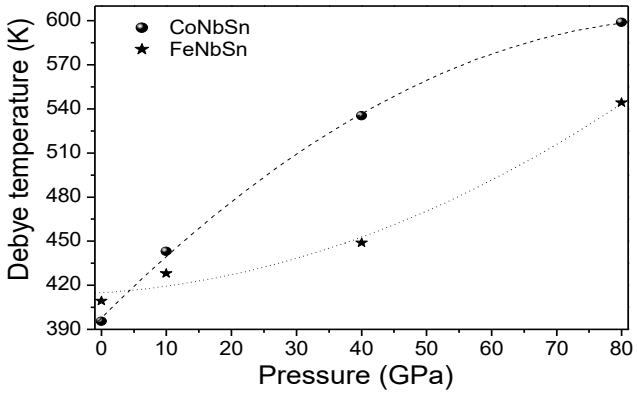

Fig. 4 – Impact of high-pressure up to 80 GPa on the Debye temperature for both CoNbSn and FeNbSn materials.

The minimum thermal conductivity k_{min} may be determined using the following equation [20]:

$$k_{min} = k_B\left[\left(\frac{nN_A\rho}{M}\right)\right]^{2/3} v_m \qquad (8)$$

The calculated k_{min} at different values of pressure (p = 0, 10, 40 and 80 GPa) for both CoNbSn and FeNbSn materials are plotted in figure 5. At zero-pressure, the minimum thermal conductivity k_{min} for FeNbSn material is 0.72 $WK^{-1}m^{-1}$, slightly higher, compared to CoNbSn, which has a lower k_{min} of around 0.70 $WK^{-1}m^{-1}$. These two laters values are very smaller than the theoretical values (2.51-2.55 $WK^{-1}m^{-1}$) reported for Silicon Carbide (SiC) polymorphs [20] and the theoretical value 2.86 $WK^{-1}m^{-1}$ reported for cubic rock-salt aluminum nitride (AlN) material [21].

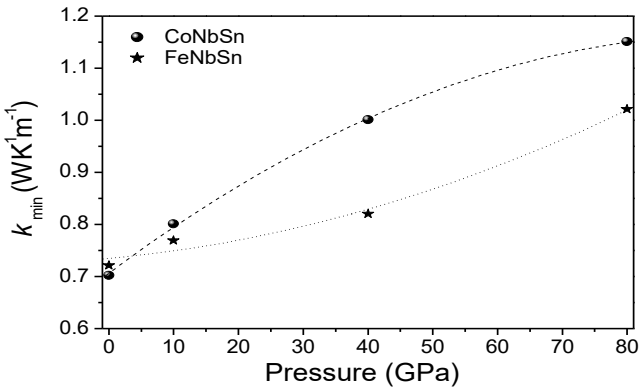

Fig. 5 – Minimum thermal conductivity k_{min} versus pressure up to 80 GPa for CoNbSn and FeNbSn materials.

2.4. Vickers hardness and Cauchy pressure

Hardness informs about the ability of a material to resist elastic or plastic deformation [19], it also informs about damage when a material is subjected to external forces [19]. It becomes necessary to predict the har-dness of materials to enable correct recommendations for technological application[4]. For several types of materials, the Vickers hardness Hv and the elastic moduli (B and G) are related by [22, 23]:

$$H_v = 2(k^2G)^{0.585} - 3 \qquad (9)$$

where the parameter k refers to the G/B ratio, B is the bulk modulus, and G is the shear modulus.

Table **2** displays the calculated Vickers hardness Hv at different values of pressure for CoNbSn and FeNbSn materials. At zero-pressure, the Hv of FeNbSn is slightly lower, reaching 9.35 GPa, compared to CoNbSn material, which has a higher Hv of 11.12 GPa. Although, this later value is higher than the theoretical ones (Hv = 7.628 and 8.914 GPa) reported by Wafula and co-authors [11], it is in excellent agreement with the theoretical values (Hv = 10.67, 11.32 and

11.89 GPa) [4]. The deviation between the values *Hv* = 11.12 and 11.32 GPa is only around 1.77%.

Table 2 – Calculated Vickers hardness *Hv* for both CoNbSn and FeNbSn materials, along with other data previously published, [a]-Ref. [4], [b]-Ref. [11] GGA, [c]-Ref. [11] LDA.

Pressure (GPa)	0	10	40	80
CoNbSn	11.12, 10.67[a] 11.32[a], 11.89[a], 7.628[b], 8.914[c]	13.93	19.33	21.83
FeNbSn	9.35	9.08	8.69	14.56

The calculated Vickers hardness *Hv* at different values of pressure for CoNbSn and FeNbSn materials are also plotted in figure 6. As for several materials [24, 25], the the Vickers hardness *Hv* of CoNbSn substances increase when the pressure increase.

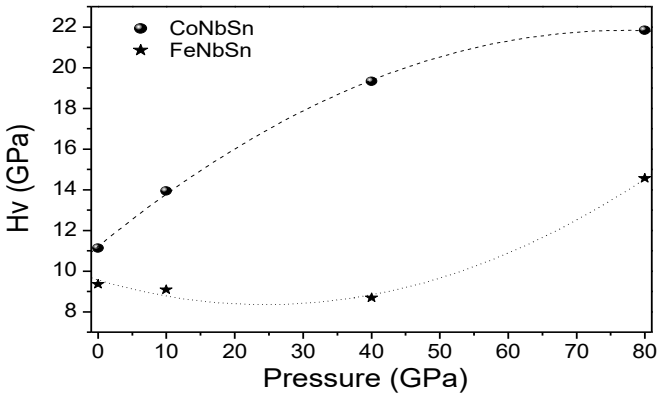

Fig. 6 – Impact of high-pressure up to 80 GPa on the Vickers hardness *Hv* for CoNbSn and FeNbSn materials.

The Cauchy pressure *Cp* in cubic crystals under pressure is given by: $C_P = C_{12} - C_{44} - 2p$, where *p* is the pressure [26]. At zero-pressure, the C_P of FeNbSn material is slightly higher, reaching 19.5 GPa, compared to CoNbSn material, which has a lower C_P = 10 GPa. In accordance with Pettifor's rule [27], a larger positive value for C_P implies a larger quantity of metallic bonds within the material and, consequently, increased toughness; vice versa, a more signifiant negative C_P value indicates an increased covalent bond number in the material [24], and thus, increased brittleness [4]. Furtherore, the deviation from C_P is a measure of the contribution from the non central many-body force considering the extended interaction potential (EIP) approach [28].

As pressure is increased from 0 to 80 GPa, it is found that the values of the *Cp* for both CoNbSn and FeNbSn materials decreases monotonically and non-linearly as shown in figure 7. The Cauchy pressure variation indicates that the brittleness of both FeNbSn and CoNbSn materials increases gradually with increasing pressure from 0 to 80 GPa. We note that a similar behavior was observed also for MgO binary oxide material [26].

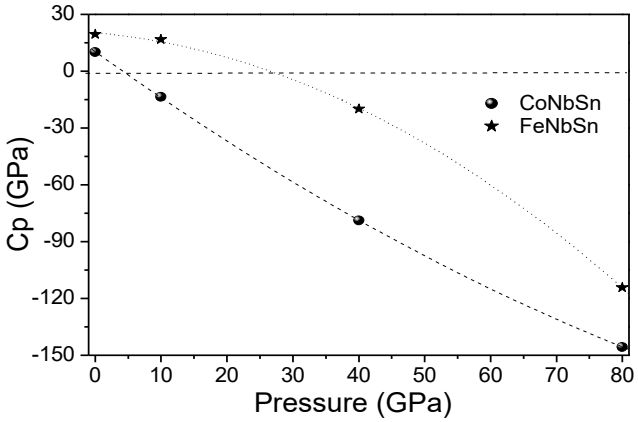

Fig. 7 – Cauchy pressure *Cp* versus pressure up to 80 GPa for CoNbSn and FeNbSn materials.

The quadratic polynomial fits of *Cp* (in GPa) as a function of pressure *p* (in GPa) are as follows:

$$Cp = 10.31 - 2.50p + 6.87 \times 10^{-3}p^2 \text{ (for CoNbSn)} \qquad (10)$$

$$Cp = 20.29 - 0.30p - 1.73 \times 10^{-2}p^2 \text{ (for FeNbSn)} \qquad (11)$$

For FeNbSn material, the decrease of *Cp* is relatively slow up to 30 GPa and then rapid between 30 and 80 GPa, as shown in figure 7.

3. CONCLUSION

In this work, we invastigate the effect of high pressure up to 80 GPa on the sound velocities, Debye temperature, minimum thermal conductivity, Vickers hardness and Cauchy pressure for both CoNbSn and FeNbSn ternary materials using theoretical structural parameters and elastic constants of the litterature.

The conclusions from the results reported in Section 2 are as follows : firstly, the zero-pressure Debye temperature for FeNbSn material is slightly higher, reaching the value 409.2 K, compared to CoNbSn semiconducting material, which has a lower θ_D of around 395.5 K. Our calculated zero-pressure sound velocity, Debye temperature and Vickers hardness for CoNbSn material are in good agreement with the theoretical values of the litterature. The deviation between our value 11.12 GPa and that 11.32 GPa of the litterature is only 1.77%. The agreement supports using these fidings as a reference for research and future applica-tions. Secondly, it is noted that the sound velocity, Debye temperature, minimum thermal conductivity, and Vickers hardness of both CoNbSn and FeNbSn materials tend to increase with increasing pressure up to 80 GPa, while the Cauchy pressure for both materials decreases with increasing pressure up to 80 GPa.

REFERENCES

1. A. Giri, P. Khatri, H. K. Neupane, N. P. Adhikari, *Mater. Res. Express* **11**, 115501 (2024).
2. M. Islam, M.A.R. Sheikh, *Physica B* **668**, 415244 (2023).

3. J. B. Gu, C. J. Wang, Y. Cheng, L. Zhang, L. C. Cai, G. F. Ji, *Comput. Mater. Sci.* **96**, 72 (2015).
4. O. E. Osafile, O. N. Nenuwe, *J. Nig. Soc. Phy s. Sci.* **3**, 121 (2021).
5. R. M. Shabara and B. O. Alsobhi, *Rev. Mex. Fís.* **70**, 041002 (2024).
6. W. J. Tropf, M. F. Thomas, T. J. Harris, *Properties of crystals and glasses*, *Handbook of Optics,* Vol. IV, (McGraw-Hill, New York, 2004).
7. S. Daoud, N. Bioud, N. Lebga, *J. Optoelectron. Adv. M.* **16**, **No. 1-2**, 207 (2014).
8. M. Güler, E. Güler, *Crystals* **7**, 164 (2017).
9. J. Zhou, J. Lian, Y.C. Ding, Y. Gao, W. Zhu, *Results Phys.* 14, 102453 (2019).
10. S. Daoud, N. Bioud, L. Belagraa, N. Lebga, *J. Nano- Electron. Phys.* **5**, 04061 (2013).
11. J. W. Wafula, J. W. Makokha, and G. S. Manyali, *Results Phys.* 43, 106132 (2022).
12. B. Gurunani, D. C. Gupta, *RSC Adv.* **15**, 4874 (2025).
13. N. Bioud, N. Benchiheub, *Chem. Phys. Impact* **7**, 100342 (2023).
14. N. Benkara-Mohammed, N. Bioud, N. Benchiheub, *Comput. Condens. Matter.* **39**, e00895 (2024).
15. S. Daoud, N. Bouarissa, H. Rekab-Djabri, P. K. Saini, *Silicon* **14**, 6299 (2022).
16. N. Bioud, X.W. Sun, N. Bouarissa, S. Daoud, *Z. Naturforsch. A* **73**, 767 (2018).
17. S. Daoud, N. Bioud, N. Lebga, *Pramana J. Phys.* **81**, 885 (2013).
18. C. Toher, J. J. Plata, O. Levy, M. De Jong, M. Asta, M. B. Nardelli, S. Curtarolo, *Phys. Rev. B* **90**, 174107 (2014).
19. C. Xiao, L. Liu, S. Liu *et al.*, *Metals* **14**, 789 (2024).
20. M. Islam, Nucl. Mater. Energy **38**, 101631 (2024).
21. N. Lebga, S. Daoud, X-W Sun, N. Bioud, A. Latreche, *J. Electron Mater.* **47**, 3430 (2018).
22. X. Q. Chen, H. Niu, D. Li, and Y. Li, *Intermetallics* **19**, 1275 (2011).
23. B. O. Mnisi, E. M. Benecha, M. M. Tibane, *Mater. Adv.* **5**, 5632 (2024).
24. C. Xiao, B. Yang, Z. Lai *et al.*, *Crystals* **15**, 3 (2025).
25. Z.-X. Yang, X.-Y. Kuang, Z.-H. Wang, M.-M. Zhong, X.-F. Huang, *Solid State Sci.* **28**, 20 (2014).
26. B. B. Karki, G. J. Ackland, J. Crain, *J. Phys. Condens. Matter*. **9**, 8579 (1997).
27. D. Pettifor, *Mater. Sci. Technol.* **8**, 345 (1992).
28. P. Bhardwaj, S. Singh, *Mater. Chem. Phys.* **125**, 440 (2011).